IEEE Photonics Journal
An IEEE Photonics Society Publication

Open Access

Tunable S-Band Q-Switched Fiber Laser Using Bi_2Se_3 as the Saturable Absorber

Volume 7, Number 3, June 2015

H. Ahmad
M. R. K. Soltanian
Leila Narimani
I. S. Amiri
A. Khodaei
S. W. Harun

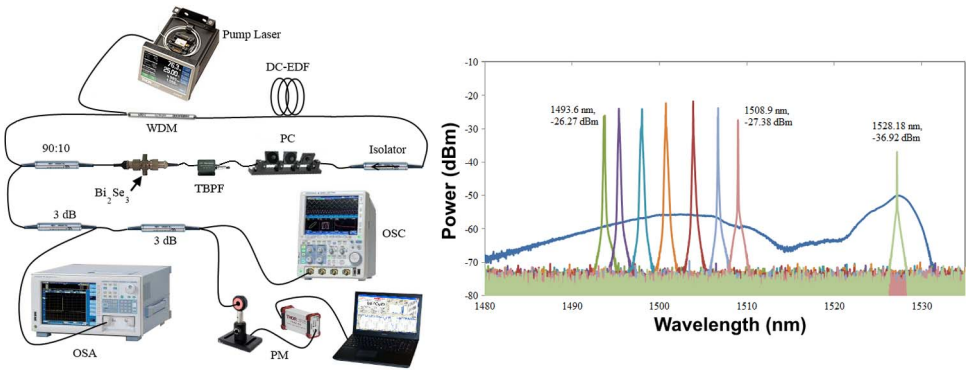

DOI: 10.1109/JPHOT.2015.2433020
1943-0655 © 2015 IEEE

IEEE photonics SOCIETY

IEEE

Tunable S-Band Q-Switched Fiber Laser Using Bi_2Se_3 as the Saturable Absorber

H. Ahmad,[1] M. R. K. Soltanian,[1] Leila Narimani,[2] I. S. Amiri,[1] A. Khodaei,[1] and S. W. Harun[1]

[1]Photonics Research Centre, University of Malaya, Kuala Lumpur 50603, Malaysia
[2]Chemistry Department, Faculty of Science, University of Malaya, Kuala Lumpur 50603, Malaysia

DOI: 10.1109/JPHOT.2015.2433020

Manuscript received April 28, 2015; accepted May 12, 2015. Date of publication May 13, 2015; date of current version May 28, 2015. This work was supported by the University of Malaya/MOHE under Grant UM.C/625/1/HIR/MOHE/SCI/29. Corresponding author: H. Ahmad (e-mail: harith@um.edu.my).

Abstract: This paper describes a successful demonstration of S-band region wavelength output generated via a tunable Q-switch fiber laser with the topological insulator (TI) Bi_2Se_3 as a saturable absorber (SA). The modulation depth of the TI was measured as 11.1%, whereas the utilized 980-nm laser source operated at 100 mW pump power. By inserting the TI-SA between two ferrules and utilizing a tunable bandpass filter (TBPF), a stable and tunable Q-switching operation was achieved over the S-band wavelength region from 1493.6 to 1508.9 nm, wherein pulsewidth was 7.6 μs, and the tunable repetition rate ranged from 26.1 to 36.6 kHz. The Q-switched pulses had maximum pulse energy of 6.1 nJ, as measured from 2.5% of the cavity output. The results provide evidence that a TI-based SA is suitable for pulsed laser operation in the S-band wavelength region and offers potential for further development as an ultrabroadband photonics device.

Index Terms: Topological insulator saturable absorber (TI-SA), bismuth Bi_2Se_3, tunable S-band Q-switched fiber laser, depressed cladding erbium-doped fiber laser (DC-EDF).

1. Introduction

The generation of ultrafast pulses has been recently demonstrated via mode-locked fiber lasers with a saturable absorber (SA) of graphene [1]–[7], carbon nanotube (CNT) [8], [9], or graphene oxide [10], [11], as well as a variety of gain media involving dopants such as erbium (Er^{3+}), ytterbium (Yb^{3+}), and thulium (Tm^{3+}). Generally, in mode locking, the random phase relationship arising from the oscillations of various modes can be manipulated via a SA, which results in a train of ultrashort pulses that vary in duration from picoseconds to a few tens of femtoseconds. These ultrashort pulses are useful for many applications, especially within the area of chemical analysis, molecular dynamics, optical and atomic physics, as well as in laser writing in glass and also microfabrication. The design of mode-locked fiber lasers can be rather involved and requires careful balancing between the dispersion and nonlinear properties of the various intracavity components in order to achieve stable operation. There is a need for compact, inexpensive, and efficient pulse lasers for applications in material processing, environmental sensing, range finding and in medicine e.g. as a source for breaking up kidney stones. These applications require pulses with higher energy content and longer durations than those

generated from mode-locked fiber lasers, and Q-switched fiber lasers present a highly suitable means for providing such pulses.

A Q-switched fiber laser is based on modulation of the quality factor, Q (the ratio between the energy stored in the active medium and that lost per oscillation cycle), of the cavity. An SA plays an important role in providing the mechanism to generate Q-switched pulses within an efficient low cost system. There have been reports of using CNT [12], [13], graphene [14]–[18], and graphene oxide [15], [16], [19] to generate Q-switched pulses that are generally tunable. In the case of a CNT SA, the generated Q-switched pulses of [13] had pulse duration of 7 μs, average pulse repetition rate of 12 kHz, and a tunability ranging from 1555 to 1560 nm. For the case of a graphene SA, [17] reported pulse duration of 2 μs, average repetition rate of 103 kHz, and a tunability of 1522 to 1555 nm at pump power of 200 mW when using a 980 nm pump laser. Q-switched pulses can be considered from such reported works to possess pulse duration in the region of microseconds, average power of about few mW, and a repetition rate in the region of kHz that is largely dependent on the pump power. There has been interest lately of using a topological insulator (TI), such as Bi_2Se_3, as an SA within mode-locked or Q-switched fiber laser systems [20]. Results of using TI-based SAs such as MoS_2 and Bi_2Te_3 have provided indications of their unique potential for ultra-fast photonics, ranging from high-speed light modulation and ultra-short pulse generation to ultra-fast optical switching [21]–[24]. The interest in Bi_2Se_3 is due to its relatively low saturation intensity, I_{sat}, which can be very useful for developing low-threshold Q-switched or mode-locked lasers. An early report by Zhao et.al [25] describes using this TI-SA alongside erbium-doped fiber to generate Q-switched fiber lasers in 1, 1.5, and 2 μm regions [20], [26], [27]. To the best of our knowledge, there is no investigation on the generation of tunable Q-switched fiber laser output in the S-band region utilizing Bi_2Se_3, whereas most reports on SAs in comparable configurations cover single and multiwall CNT, graphene oxide and also TIs utilized in the C- and L-band regions. There are several reports [18], [28] regarding a graphene oxide SA for Q-switched operation in the S-band region, which covers from 1460 nm to 1520 nm as defined by the ITU-T standard. Continuous and rapidly growing demands on data traffic currently exist due to various recent applications, and this situation has resulted in a considerable focus on expanding the capacity of optical signal transmission. These data traffic demands have been catalyzed by the development of dense wavelength division multiplexing (WDM) transmission systems, and consequently the signal transmission in the S-band wavelength region has become critical for fulfilling traffic demands. Additionally, the generation of Q-switched pulsed lasers in this spectral region could be advantageous and result in novel applications in many fields, such as laser processing, medicine, environmental sensing, range finding, telecommunications, reflectometry, remote sensing, and material processing [29]–[31]. The main advantage of the work described in this paper, when compared to earlier reports, is the tunability of the generated Q-switched fiber laser resulting from the use of TI : Bi_2Se_3.

Passively Q-switched fiber lasers (PQFLs) generate Q-switched pulses that are applicable in the area of material processing, range findings, telecommunications and medicine. The advantage of PQFLs is the aforementioned high energy per pulse as compared to mode-locked fiber lasers, and also the possibility of a wide tuning range that can arise in the presence of various gain media as mentioned earlier. Generally, PQFLs are relatively simple in design, low cost, and provide stable and consistent output power.

Section 2 details an experimental approach to measure the modulation depth of the TI-based SA, while Section 3 provides a description of the experimental setup of the TI-SA based Q-switching fiber laser and its configuration. The experimental results and subsequent discussion of the findings is covered in Section 4. Finally, a conclusion to the outcome of this research work is given in Section 5.

2. Measuring the Modulation Depth of the TI-SA

Fig. 1(a) shows the setup utilized for measuring the modulation depth of the TI-SA. This configuration was a typical balanced twin detector measurement technology device that had a simple

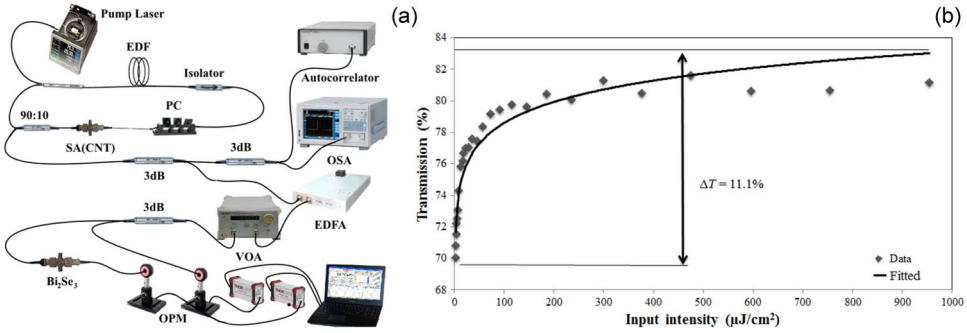

Fig. 1. (a) Configuration setup to measure the modulation depth of the TI : Bi_2Se_3 using input pulses sourced from a mode-locked laser and (b) the transmission spectrum of Bi_2Se_3 showing a depth of about 11.1%.

mode-locked laser cavity with center operation wavelength of 1560 nm incorporated instead of a market laser source. The total length of the laser cavity was approximately 12 m. Aside from the erbium-doped fiber (EDF), all fibers used in the cavity were Corning SMF-28. A 980 nm pump laser operating in continuous wave (CW) mode was connected to a 980/1550 nm WDM. This WDM was linked to a 0.9 m Leikki EDF gain medium possessing a numerical aperture of 0.21 to 0.24, a mode field diameter of 5.7–6.6 at 1550 nm, and an absorption coefficient of 84 dBm at 980 nm. The other end of this EDF was connected to an isolator that was then coupled to a polarization controller (PC). Subsequently, this PC was linked to CNTs that were sandwiched between two ferrules, whereupon this arrangement provided for a mode-locking mechanism. The other end of the ferrule was then connected to a 90:10 coupler, which allowed for extraction of a portion of the generated mode-locked laser. A subsequent extracted slice would be utilized as a pulse laser source for accurately measuring the nonlinear transmission curve of the TI : Bi_2Se_3. The 90% port was then connected to the signal port of the WDM, and this link closed the fiber laser loop. Alterations to the PC allowed for the emergence of mode-locked lasing due to the strong polarization-dependency, and this mode-locked output was used as input pulses for measuring the modulation depth of TI-SA. The mode-locked pulse laser had a width of 0.6 ps and a repetition rate of 16.6 MHz. Output power of the mode-locked laser source was adjustable. The mode-locked laser output was amplified by a homemade EDFA and passed through a variable optical attenuation (VOA) (Anristsu MN9610B). The output light was subsequently divided into two equal laser beams via a 3 dB coupler, whereupon one laser beam propagated through the Bi_2Se_3 TI-SA and was subsequently measured using a photodiode detector (Thorlabs DET01CFC), while the other laser beam was directly connected to an identical photodiode detector. In order to sufficiently suppress potential detection errors, these two detectors were connected to two power meter separately (PM-100 Thorlabs) that was configured to replicate the photodiode detector performance via tuning parameters such as integration time and detection wavelength. A series of output power and input power measurements were recorded while adjustments were made to the attenuator loss, in which the loss deviations corresponded to the variation of the input laser intensity. Consequently, the optical transmittance under different input powers could be determined via division of the output power by the input power. The resultant nonlinear transmission curve is plotted in Fig. 1(b).

The dependence of an SA nonlinear absorption behavior on the intensity of the incident beam can be described using the following simple formula [32], [33]:

$$T(I) = 1 - \Delta T \cdot \exp\left(\frac{-I}{I_{sat}}\right) - \alpha_{ns}$$

where $T(I)$ is the transmission, ΔT is the modulation depth, I is the input pulse energy, I_{sat} is the saturation energy, and α_{ns} is the nonsaturable loss. The transmission of the material rises

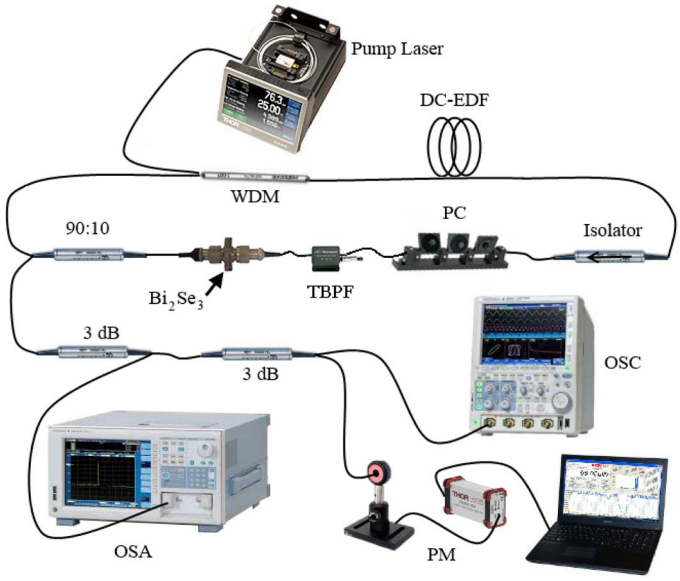

Fig. 2. Configuration setup for Q-switched pulsed laser with S-band region output.

as the incident beam intensity increases, which indicates that passive amplitude modulation of the incident beam is possible with simple laser devices. The key parameters that determine the performance of an SA are the modulation depth, nonsaturable loss, recovery time, saturation fluence, and damage threshold. Fig. 1(b) shows the nonlinear transmission curve for the Bi_2Se_3 as an SA, where the modulation depth is defined as the difference in the transmission between the nonsaturable loss and the background absorption loss (α_0). In this case, the modulation depth was observed to be 11.1%.

3. Experimental Setup

Fig. 2 shows the experimental setup for a Q-switched S-band depressed cladding erbium-doped fiber (DC-EDF) laser that could be tuned from 1493.6 nm to 1508.9 nm as permitted by the tunable band pass filter (TBPF). A wider range of tunability is achievable if the spectral response of the selectable tunable filter can accommodate the range of the amplified spontaneous emission (ASE) spectrum of the S-band EDF. The ASE in this experiment covered 1480 nm to 1530 nm, as shown in the blue color within Fig. 5(a). The pump laser used in this experiment was a 974 nm laser diode capable of generating maximum output of 600 mW, and was coupled to a 980/1530 WDM. The output port of this WDM was subsequently connected to a 15 m length of DC-EDF. The S-band EDF inside the amplifier module had a depressed cladding design in order to provide a long wavelength cutoff filter for the fundamental mode (near 1530 nm) of the fiber. Specifications of the DC-EDF included an absorption coefficient of 7.6 dB/m in 974 nm, a core composition of approximately 2.5% GeO_2, 5.5% Al_2O_3, 92% SiO_2, and 0.15 wt.% erbium, and a depressed cladding composition of approximately 3% Fluorine, 0.5% P_2O_5, and 96.5% SiO_2. The numerical aperture of the core was 0.22. The other end of the fiber was fusion-spliced to an optical isolator that was, in turn, connected to a PC used for optimizing the Q-switched operation of the fiber laser. The output port of the PC was linked to a TBPF, which was then coupled with a Q-switched device consisting of a Bi_2Se_3 layer placed between two ferrules. The output connection was spliced to a fused biconical 90 : 10 coupler, with the 90% port attached to the signal port of the WDM. The 10% port of the coupler was connected to two 3-dB fused conical couplers in order to facilitate a real-time monitoring of the Q-switched pulsed laser via an oscilloscope (YOKOGAWA DLM2050), spectrum of the laser via an optical spectrum analyzer (OSA) (YOKOGAWA AQ6370B) with a spectral range of 600–1700 nm and resolution of 0.02 nm, and measurements of the average

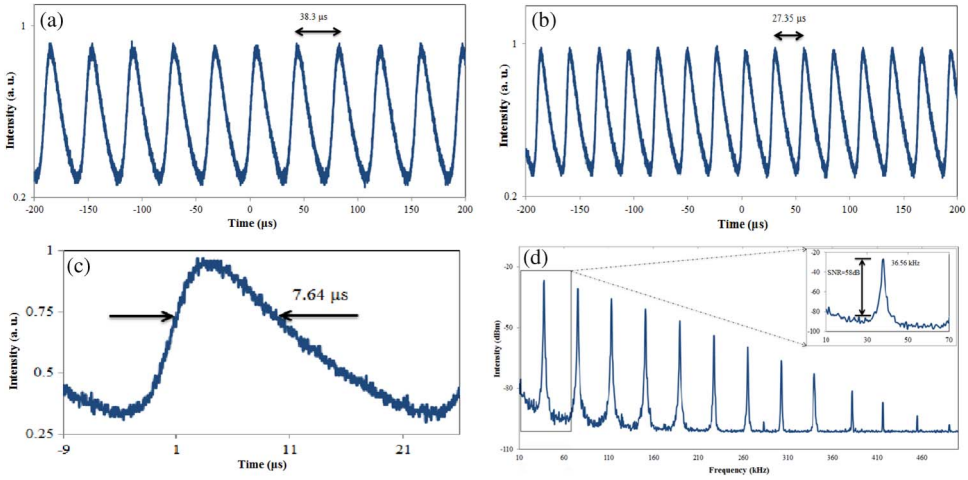

Fig. 3. Oscilloscope trace of the Q-switched pulse train for (a) pump power of 60 mW, (b) pump power of 100 mW, and (c) single pulse envelope with pulse width of 7.64 μs, along with (d) RF output spectrum and the relevant harmonics. The inset in (d) shows the main harmonic with SNR of 58 dB.

output power via a Thorlabs PM-100 power meter. The experimental setup allowed for a flexible Q-switched operation that employed Bi_2Se_3 as an SA and tunability ranging from 1493.6 nm to 1508.9 nm.

4. Results and Discussions

The Q-switched fiber laser output began at a minimum pump power of 60 mW, whereupon the pulses had a repetition rate of 26.1 kHz that corresponded to a pulse period of 38.3 μs, as shown in Fig. 3(a). Fig. 3(b) shows a pulse period of 27.3 μs in relation to the pump power of 100 mW, and a repetition rate of 36.6 kHz is observable from the radio-frequency (RF) trace frequency spectrum in Fig. 3(d). The achieved signal-to-noise ratio (SNR) of 58 dB, as can be observed from the inset of Fig. 3(d), was comparable or superior to that attained by a number of passively Q-switched lasers in previously mentioned reports [17], [27], [34]. Fig. 3(c) shows the pulse width of 7.6 μs. The rise time of the pulse shape, as shown in Fig. 3(c), is proportional to the net gain after the Q-value of the cavity is switched to a high value. The light intensity growth is proportional to $2g_0/T_R$ [35], [36], where g_0 is small signal gain and $T_R = 2L/C_0$ is the round-trip-time in a linear cavity with optical length $2L$ or a ring cavity with optical length L. An output coupler with transmission T_{out} and output coupling coefficient l_{out} has the definition $T_{out} = 1 - \exp(-l_{out})$, and a parasitic loss coefficient that is l_p. l_{out} and l_p determine the total nonsaturable loss coefficient per round trip, $l = l_{out} - l_p$. When the gain is depleted, the fall time is mostly dependent on the cavity decay time τ_p. A short cavity length, high gain and a large change in the cavity Q is necessary for short Q-switched pulses. If the Q-switch is not fast, the pulse width can become limited by the speed of the switch. Consequently, for $l < q_0$ the pulses become asymmetric.

An increase in pump power from 60 mW to 100 mW resulted in the repetition rate of the Q-switched pulses becoming tuned from 26.1 kHz to 36.6 kHz, with a corresponding decrease in pulse width from 38.3 μs to 27.3 μs. The pulse width could be further narrowed by optimizing parameters such as cavity length or modulation depth of the TI : Bi_2Se_3 Q-switcher [27].

Fig. 4(a) shows the pulse width and pulse repetition rate as a function of the pump power. Increasing the pump power from 60 to 100 mW linearly increased the repetition rate. Pulse width decreased rapidly as the pump power was increased from 60 to 73 mW, and then decreased monotonically while pump power increased from 78 to 100 mW. Fig. 4(b) illustrates the average output power and the pulse energy as a function of the pump power. The pulse energy increased almost linearly as the pump power increased, and the average output power likewise

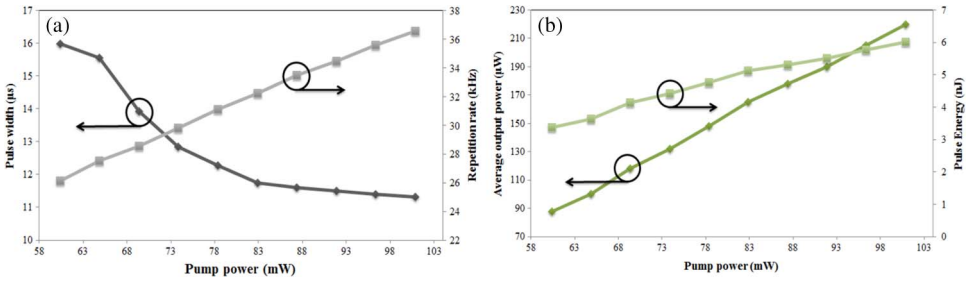

Fig. 4. (a) Pulse width and pulse repetition rate as a function of pump power and (b) average output power and pulse energy as a function of pump power.

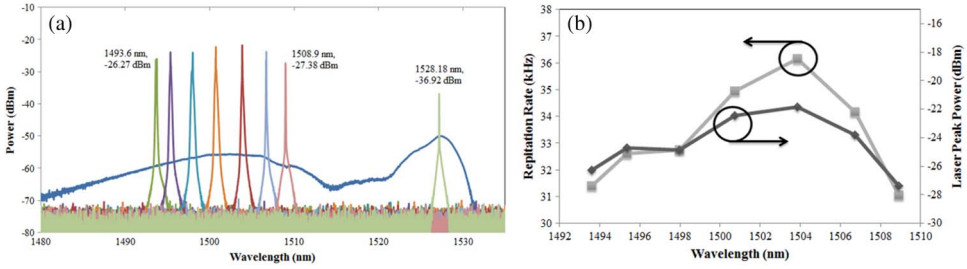

Fig. 5. (a) Lasing achieved by tuning the TBPF and S-band ASE spectrum (shown in blue) and (b) repetition rate and laser peak power as a function of wavelength at a constant pump power of 100 mW.

showed a similar relationship with pump power. These graphs were based on results acquired from output that had been split by two successive 3-dB couplers that were in turn connected to the 10% output portion of the ring cavity. The maximum obtained pulse energy of 6.1 nJ, achieved from 2.5% of the cavity output, is shown in Fig. 4(b), although higher levels of energy would have been circulating in the cavity. The Q-switched pulse width is obtained by dividing the pulse energy by its maximum power [37], expressed as

$$\tau_s \approx \frac{r_{in}\eta_{ext}/\zeta}{r_{in} - 1 - \ln r_{in}} \times \tau_c$$

where r_{in} is the initial inversion ratio, τ_c is the cavity lifetime, and ζ is the maximum achievable extraction efficiency. The extraction efficiency η_{ext} of the stored energy by the Q-switched pulse depends solely on the inversion ratio and is determined implicitly by the following equation [37]:

$$r_{in} = \frac{1}{\eta_{ext}/\zeta} \ln\left[\frac{1}{1 - \eta_{ext}/\zeta}\right]$$

The extraction efficiency increases monotonically with the inversion ratio. The pulse width scales similarly to that for the photon cavity lifetime, and thus is proportional to the cavity length. The pulse width decreases rapidly at small inversion ratios, yet changes slowly as the inversion ratio increases. Pulse duration could be further narrowed by shortening the cavity length and improving the modulation depth of the Bi_2Se_3 SA [36]. By increasing the pump power from 78 to 100 mW, as shown in Fig. 4(a), the pulse width decreased monotonically from 12.28 μs to 11.32 μs.

Fig. 5(a) illustrates the tunability of the lasing in the S-band region for 8 tuned wavelengths whilst pump power is kept constant at 100 mW. Average 3-dB bandwidth for each lasing output spectrum was approximately 0.017 nm, and the laser could be tuned from 1485 nm to 1530 nm,

which was limited to the loss of the tunable filter and ASE across the S-band gain medium. The ASE is shown in blue in Fig. 5(a). Although lasing can be achieved along the ASE range from 1485 nm to 1530 nm, lasing in the Q-switching mechanism was triggered at a wavelength of 1493.6 nm with a corresponding output peak power of -26.27 dBm. There were also Q-switched outputs at a wavelength of 1508.9 nm and measured power of −27.38 dBm. No Q-switched pulses occurred above this wavelength, and this absence was due primarily to the insertion loss of the TBPF and the gain of the ASE not supporting Q-switched pulsing at the low pump power used in this set up. Lasing with Q-switched output in this region would occur if the pump power were to be increased beyond 100 mW. Slowly shifting the TBPF to higher wavelengths meant that the lasing peak power was followed by the gain of the ASE, as shown in Fig. 5(b), and the laser peak power varied as a function of wavelength. The achieved Q-switched pulses had maximum pulse energy of 6.1 nJ as measured from 2.5% of the cavity output. A very limited number of suitable low loss devices operate in the S-band region. The tunability range very much depends on the bandwidth and loss of the tunable bandpass filter (TBPF) used in the set up. A wider tunability in S-band region can be achieved by using a TBPF with lower loss and higher bandwidth to cover the whole S-band region. Consequently, a higher energy of Q-switching pulses is a result of utilizing a higher gain medium and low loss devices.

Fig. 5(b) also shows the repetition rate and laser peak power as a function of wavelength, for which the wavelength was tuned via TBPF adjustments. Fig. 5(b) displays 7 points, each of which represents the corresponding lasing wavelength shown in Fig. 5(a) and their repetition rate. The repetition rate of the achieved Q-switched fiber laser was relatively related with the laser peak power. Tuning the TBPF allowed for lasing at the higher wavelength of 1528.17 nm, as shown in Fig. 5(a), without Q-switching, although increasing the pump power would assuredly have resulted in Q-switched pulse output.

5. Conclusion

A simple, tunable Q-switched fiber laser using a TI-SA for S-band wavelength operation has been experimentally demonstrated for the first time to the best of the authors' knowledge. The laser cavity consisted of a 15 m length of DC-EDF, a TBPF, and a TI-based SA composed of Bi_2Se_3 that was sandwiched between two ferrules. The passive Q-switching operation produced pulses with a minimum pulse width of 7.64 μs and a tunable repetition rate ranging from 26.12 to 36.56 kHz. These performances are competitive with those reported for Q-switched fiber lasers utilizing other SAs, such as graphene, CNT, or graphene oxide, and could be further improved by optimizing the cavity design and purity of the TI sample. Moreover, the modulation depth of the TI was investigated and measured carefully; a modulation depth of 11.1% was achieved. The success of this research work can provide a foundation for further design improvements and applications.

References

[1] Z. Sun *et al.*, "Graphene mode-locked ultrafast laser," *ACS Nano*, vol. 4, no. 2, pp. 803–810, Feb. 2010.
[2] H. Zhang, D. Tang, L. Zhao, Q. Bao, and K. Loh, "Large energy mode locking of an erbium-doped fiber laser with atomic layer graphene," *Opt. Exp.*, vol. 17, no. 20, pp. 17 630–17 635, Sep. 2009.
[3] Y.-W. Song, S.-Y. Jang, W.-S. Han, and M.-K. Bae, "Graphene mode-lockers for fiber lasers functioned with evanescent field interaction," *Appl. Phys. Lett.*, vol. 96, no. 5, Feb. 2010, Art. ID. 051122.
[4] H. Ahmad, M. Soltanian, C. Pua, M. Alimadad, and S. Harun, "Photonic crystal fiber based dual-wavelength Q-switched fiber laser using graphene oxide as a saturable absorber," *Appl. Opt.*, vol. 53, no. 16, pp. 3581–3586, Jun. 2014.
[5] H. Ahmad, M. Soltanian, M. Alimadad, and S. Harun, "Stable narrow spacing dual-wavelength Q-switched graphene oxide embedded in a photonic crystal fiber," *Laser Phys.*, vol. 24, no. 10, Mar. 2014, Art. ID. 105101.
[6] G. Lin and Y. Lin, "Directly exfoliated and imprinted graphite nano-particle saturable absorber for passive mode-locking erbium-doped fiber laser," *Laser Phys. Lett.*, vol. 8, no. 12, pp. 880–886, Dec. 2011.
[7] Y. Lin and G. Lin, "Free-standing nano-scale graphite saturable absorber for passively mode-locked erbium doped fiber ring laser," *Laser Phys. Lett.*, vol. 9, vol. 5, pp. 398–404, May 2012.
[8] A. G. Rozhin *et al.*, "Sub-200-fs pulsed erbium-doped fiber laser using a carbon nanotube-polyvinylalcohol mode locker," *Appl. Phys. Lett.*, vol. 88, no. 5, Jan. 2006, Art. ID. 051118.

[9] V. Scardaci *et al.*, "Carbon nanotube polycarbonate composites for ultrafast lasers," *Adv. Mater.*, vol. 20, no. 21, pp. 4040–4043, Nov. 2008.
[10] J. Xu, J. Liu, S. Wu, Q.-H. Yang, and P. Wang, "Graphene oxide mode-locked femtosecond erbium-doped fiber lasers," *Opt. Exp.*, vol. 20, no. 14, pp. 15 474–15 480, Jul. 2012.
[11] J. Zhao *et al.*, "An L-band graphene-oxide mode-locked fiber laser delivering bright and dark pulses," *Laser Phys.*, vol. 23, no. 7, Jul. 2013, Art. ID. 075105.
[12] S. Harun *et al.*, "A Q-switched erbium-doped fiber laser with a carbon nanotube based saturable absorber," *Chin. Phys. Lett.*, vol. 29, no. 11, Nov. 2012, Art. ID. 114202.
[13] D.-P. Zhou, L. Wei, B. Dong, and W.-K. Liu, "Tunable passively-switched erbium-doped fiber laser with carbon nanotubes as a saturable absorber," *IEEE Photon. Technol. Lett.*, vol. 22, no. 1, pp. 9–11, Jan. 2010.
[14] J. Liu, S. Wu, Q.-H. Yang, and P. Wang, "Stable nanosecond pulse generation from a graphene-based passively *Q*-switched Yb-doped fiber laser," *Opt. Lett.*, vol. 36, no. 20, pp. 4008–4010, Oct. 2011.
[15] Z. Luo *et al.*, "Graphene-based passively Q-switched dual-wavelength erbium-doped fiber laser," *Opt. Lett.*, vol. 35, no. 21, pp. 3709–3711, Nov. 2010.
[16] G. Sobon *et al.*, "Linearly polarized, Q-switched Er-doped fiber laser based on reduced graphene oxide saturable absorber," *Appl. Phys. Lett.*, vol. 101, no. 24, Dec. 2012, Art. ID. 241106.
[17] D. Popa *et al.*, "Graphene Q-switched, tunable fiber laser," arXiv preprint: *arXiv:1011.0115*, 2010.
[18] H. Ahmad, M. Zulkifli, F. Muhammad, A. Zulkifli, and S. Harun, "Tunable graphene-based Q-switched erbium-doped fiber laser using fiber Bragg grating," *J. Mod. Opt.*, vol. 60, no. 3, pp. 202–212, Feb. 2013.
[19] Y. Yap, N. Huang, S. Harun, and H. Ahmad, "Graphene oxide-based Q-switched erbium-doped fiber laser," *Chin. Phys. Lett.*, vol. 30, no. 2, Feb. 2013, Art. ID. 024208.
[20] Y. Chen *et al.*, "Self-assembled topological insulator: Bi_2Se_3 membrane as a passive Q-switcher in an erbium-doped fiber laser," *J. Lightw. Technol.*, vol. 31, no. 17, pp. 2857–2863, Sep. 2013.
[21] Y.-H. Lin *et al.*, "Soliton compression of the erbium-doped fiber laser weakly started mode-locking by nanoscale p-type Bi2Te3 topological insulator particles," *Laser Phys. Lett.*, vol. 11, no. 5, May 2014, Art. ID. 055107.
[22] S. Chen *et al.*, "Broadband optical and microwave nonlinear response in topological insulator," *Opt. Mater. Exp.*, vol. 4, no. 4, pp. 587–596, Apr. 2014.
[23] J. Du *et al.*, "Ytterbium-doped fiber laser passively mode locked by few-layer molybdenum disulfide (MoS2) saturable absorber functioned with evanescent field interaction," *Sci. Rep.*, vol. 4, Sep. 2014, Art. ID. 6346.
[24] H. Zhang *et al.*, "Molybdenum disulfide (MoS 2) as a broadband saturable absorber for ultra-fast photonics," *Opt. Exp.*, vol. 22, no. 6, pp. 7249–7260, Mar. 2014.
[25] C. Zhao *et al.*, "Wavelength-tunable picosecond soliton fiber laser with topological insulator: Bi_2Se_3 as a mode locker," *Opt. Exp.*, vol. 20, no. 25, pp. 27 888–27 895, Dec. 2012.
[26] Z. Luo *et al.*, "1.06 μm Q-switched ytterbium-doped fiber laser using few-layer topological insulator Bi_2Se_3 as a saturable absorber," *Opt. Exp.*, vol. 21, no. 24, pp. 29 516–29 522, Dec. 2013.
[27] Z. Luo *et al.*, "Topological-insulator passively Q-switched double-clad fiber laser at 2 μm wavelength," *IEEE J. Sel. Topics Quantum Electron*, vol. 20, no. 5, Sep./Oct. 2014, Art. ID. 0902708.
[28] F. Muhammad, M. Zulkifli, and H. Ahmad, "Graphene based Q-switched tunable S-band fiber laser incorporating arrayed waveguide gratings (AWG)," *J. Nonlinear Opt. Phys. Mater.*, vol. 23, no. 1, Mar. 2014, Art. ID. 1450004.
[29] S. Garnov, V. Konov, T. Kononenko, V. Pashinin, and M. Sinyavsky, "Microsecond laser material processing at 1.06 μm," *Laser Phys.*, vol. 14, no. 6, pp. 910–915, 2004.
[30] H. Shangguan, L. W. Casperson, and S. A. Prahl, "Microsecond laser ablation of thrombus and gelatin under clear liquids: Contact versus noncontact," *IEEE J. Sel. Topics Quantum Electron.*, vol. 2, no. 4, pp. 818–825, Dec. 1996.
[31] M. Siniaeva *et al.*, "Laser ablation of dental materials using a microsecond Nd:YAG laser," *Laser Phys.*, vol. 19, no. 5, pp. 1056–1060, May 2009.
[32] F. Kartner, I. Jung, and U. Keller, "Soliton mode-locking with saturable absorbers," *IEEE J. Select. Topics Quantum Electron.*, vol. 2, no. 3, pp. 540–556, Sep. 1996.
[33] J. Jeon, J. Lee, and J. H. Lee, "Numerical study on the minimum modulation depth of a saturable absorber for stable fiber laser mode locking," *J. Opt. Soc. Amer. B, Opt. Phys.*, vol. 32, no. 1, pp. 31–37, Jan. 2015.
[34] J. Liu *et al.*, "Mode-locked 2 μm thulium-doped fiber laser with graphene oxide saturable absorber," presented at the CLEO: Sci. and Innovations Conf., San Jose, CA, USA, 2012, Paper JW2A.76.
[35] R. K. Willardson and A. C. Beer, *Semiconductors & Semimetals*, vol. 12, San Diego, CA, USA: Academic, 1977.
[36] G. Spühler *et al.*, "Experimentally confirmed design guidelines for passively Q-switched microchip lasers using semiconductor saturable absorbers," *J. Opt. Soc. Amer. B, Opt. Phys.*, vol. 16, no. 3, pp. 376–388, Mar. 1999.
[37] M. J. Digonnet, *Rare-Earth-Doped Fiber Lasers and Amplifiers, Revised and Expanded*. Boca Raton, FL, USA: CRC, 2002.